Antiangiogenic Effect of Docetaxel and Everolimus as Individual and Dual-Drug-Loaded Micellar Nanocarriers

Citation	Mishra, G. P., Doddapaneni, B. S., Nguyen, D., & Alani, A. W. (2014). Antiangiogenic Effect of Docetaxel and Everolimus as Individual and Dual-Drug-Loaded Micellar Nanocarriers. Pharmaceutical Research, 31(3), 660-669. doi:10.1007/s11095-013-1188-z
DOI	10.1007/s11095-013-1188-z
Publisher	Springer
Version	Accepted Manuscript
Terms of Use	http://cdss.library.oregonstate.edu/sa-termsofuse

Antiangiogenic effect of Docetaxel and Everolimus as individual and dual-drug loaded micellar nanocarriers

Gyan P. Mishra, Bhuvana Shyam Doddapaneni, Duc Nguyen and Adam WG Alani*

Department of Pharmaceutical Sciences, College of Pharmacy, Oregon State University, Corvallis, OR, USA.

*Corresponding author:

Adam Alani, Ph.D.,

Division of Pharmaceutical Sciences,

College of Pharmacy,

Oregon State University,

Corvallis, OR, 97331.

ABSTRACT

Purpose

The *in vitro* inhibitory effect of Docetaxel (DTX) and Everolimus (EVR) alone and together in poly(ethylene glycol)-*block*-poly(D,L-lactic acid) (PEG-*b*-PLA) nanocarriers on angiogenic processes and acute toxicity in mice was evaluated.

Methods

PEG-*b*-PLA DTX and/or EVR nanocarriers were characterized for size, drug loading, stability, and drug release. Cell proliferation, tubule formation, and migration studies were performed in Human Umbilical Vein Endothelial Cells (HUVEC) and Maximum Tolerated Doses (MTD) studies were in mice.

Results

DTX and EVR loading was 1.93 and 2.00 mg/mL respectively with similar solubilities for dual-drug micelles. All micelles were below 30 nm with diffusion controlled drug release. The IC_{50s} for DTX, EVR micelles were, 6.80 ± 0.67, 18.57 ± 2.86 and 0.65 ± 0.11 nM respectively with a synergistic inhibitory effect for dual-drug nanocarriers. Significant inhibition of tube formation occurred upon treatment with dual-drug nanocarriers as compared to individual micelles**.** EVR presence in dual-drug nanocarriers was able to significantly increase the inhibition of the migration of HUVEC by DTX. The MTDs for EVR, DTX and dual-drug micelles were 50, 30 and 20 mg/kg for each respectively.

Conclusions

DTX-EVR dual-drug nanocarriers have antiangiogenic effects *in vitro* mediated through cellular angiogenic process and possess clinically relevant MTD.

Keywords: Antiangiogenesis, polymeric micelles, combination therapy

INTRODUCTION:

Angiogenesis is the process of forming new blood vessels from a pre-existing vascular bed (1). In angiogenesis-dependent diseases the body losses control over angiogenesis resulting in excessive or insufficient growth of new blood vessels (2-4). Excessive angiogenesis occurs in diseases such as cancer, diabetic blindness, age-related macular degeneration, rheumatoid arthritis, psoriasis and more than 70 other conditions (4). In these conditions, new blood vessels feed diseased tissue, destroy normal tissue and in the case of cancer, angiogenesis allows tumor metastases. Excessive angiogenesis occurs when diseased cells produce an abnormal amount of angiogenic growth factors such as VEGF, PDGF, FGF and EGF resulting in minimizing the effect of endogenous angiogenesis inhibitors such as angiostatin, endostatin, thrombospondin-1, to name a few. (3). Antiangiogenic therapies are used to treat these conditions by inhibiting or slowing down new blood vessel formation and growth. Currently the Food and Drug Administration has approved thirteen drugs in the United States for cancer treatment with significant antiangiogenic activities. These drugs affect tumor angiogenesis by interfering with cell signaling pathways that are essential for angiogenic and proliferation processes. The use of antiangiogenic drugs for cancer treatment was heralded as a new treatment modality due to the lower anticipated tumor-acquired resistance over time (5). Unfortunately, clinical experience has demonstrated that acquired resistance to antiangiogenic therapeutic strategies is possible since many patients whose tumors initially respond to drugs such as bevacizumab, sorafenib, or sunitinib become nonresponsive, often within months of therapy initiation (6). The resistance to antiangiogenic drugs in cancer patients has triggered the need to establish a new treatment scheme that can actively target angiogenesis in the cancer without acquiring resistance.

One approach to overcome this resistance is the implementation of co-targeting strategies, where multiple mechanisms of drug action can target neovascular angiogenic endothelial cells within the cancer tissue. Some of the chemotherapeutic drugs such as taxanes and mammalian target of rapamycin (mTOR) inhibitors have both cytotoxic and secondary antiangiogenic effects in tumor tissues. However, their antiangiogenic capacities are not fully manifested, due in large part to limitations in dosing regimens and available drug formulations (7-10). Docetaxel (DTX) and Everolimus (EVR) a microtubule-stabilizing agent and an allosteric mTOR inhibitor respectively, are chemotherapeutic agents that have been approved in the U.S. for the treatment of multiple cancers. Both compounds individually have shown strong antiangiogenic effect in *in vitro* and *in vivo* models as well as in the clinical setting. However, the combined antiangiogenic response of DTX and EVR has neither been examined *in vitro* nor *in vivo* models.

Taxanes including DTX are among the most potent antiangiogenic chemotherapeutic agents, this effect is manifested in the human endothelial cells which are extremely sensitive to these compounds at ultra-low concentrations that have no effect on other cell type such as tumor cells, fibroblast, epithelial cells or smooth muscle cells (11-13). At these non-cytotoxic concentrations DTX appeared to inhibit VGEF induced endothelial cell migration by the reduction of the cytoplasmic chaperone *Heat-Shock protein 90* through the induction of its proteasomal degradation (14). EVR has shown antiangiogenic effect in *in vitro* and *in vivo* nonclinical models (15, 16). At the molecular levels EVR can block angiogenesis by inhibiting of hypoxia-inducible transcription in factors-1-alfa (H1Fα) translation as well as by intercepting vascular endothelial growth factor (VEGF/VEGFR) and or platelet-derived growth factor (PDGF/PDGFR) signaling cascade (17).

Polymeric micelles are colloidal particles with a size usually within the range of 15-150 nm (18). Over the last twenty years polymeric micelles have emerged as viable drug delivery system for poorly water-soluble drugs especially for cancer therapy (18, 19). Currently there are five polymeric micellar formulations for cancer therapy under clinical trials (19). Recently new drug delivery systems based on PEG-*b*-PLA polymeric micelles have been developed for the concurrent delivery of multiple anticancer drugs. These multi-drug loaded micelles have shown a synergistic inhibition of different cancers models *in vitro* and *in vivo* (20-22). Both DTX and EVR are poorly water-soluble compounds with intrinsic water solubilities at 1.9 and 9.6 µg/mL respectively (23, 24). PEG-*b*-PLA micelles can provide a unique platform as a nanocarrier for DTX (20, 25) and EVR individually and in combination. These nanocarriers can fulfill the requirements for DTX and EVR solubilization and as a delivery system for these drugs individually and in combination for the treatment of excessive angiogenesis in cancer and other diseases.

The goal of this work is to formulate PEG-*b*-PLA micellar nanocarriers for the delivery of DTX and EVR individually and in combination and evaluate their antiangiogenic activity *in vitro* on three cellular processes that essential for angiogenesis which include proliferation, tube formation and migration (26, 27). In addition, we aim to evaluate the acute toxicity of these nanocarriers *in vivo*. We *hypothesize* that DTX and EVR individual micellar nanocarriers will exert antiangiogenic effect and a synergistic effect for the dual-drug loaded nanocarriers. In addition, all micellar nanocarriers will show no acute toxicity *in vivo* at therapeutically relevant concentrations.

MATERIALS AND METHODS:

Materials

DTX and EVR were purchased from LC Laboratories (Woburn, MA). HUVEC cells and endothelial growth medium 2 were purchased from PromoCell (Heidelberg, *Germany*). Cells were cultured as per the manufacturer instructions and all experiments were performed between passages 2 and 6. Diblock copolymers PEG_{2000}-*b*-PLA_{1800} (Mn = 3800, Mw = 4100 and PI = 1.1) and PEG_{4000}-*b*-PLA_{2200} (Mn = 6100, Mw = 6500 and PI = 1.06) were purchased from Advanced Polymer Materials Inc. (Montreal, CAN). CellTiter-Blue® Cell Viability Assay kit and Apo-ONE® Homogeneous Caspase-3/7 Assay kit were obtained from Promega Inc. (Madison, WI). All other reagents of analytical grade were purchased from VWR International, LLC (Radnor, PA) and Fisher Scientific Inc. (Fairlawn, NJ).

Preparation of drug loaded micelles

DTX, EVR and DTX-EVR dual-drug loaded PEG-*b*-PLA micelles (DDM) were prepared by solvent casting method as reported previously (20, 21, 25, 28). Briefly, for the preparation of DTX or EVR individual micelles, 15 mg polymer (PEG_{2000}-*b*-PLA_{1800}) and 2 mg of DTX or EVR was dissolved in 0.5 ml of acetonitrile, which was evaporated under reduced pressure to form a thin polymeric film. Micelles were obtained by rehydration of polymeric film with 0.5 ml deionized water and then micellar solution was filtered using a 0.45 μm filter. For the DDM, DTX (2 mg) and EVR (2 mg), and PEG_{2000}-*b*-PLA_{1800} (15 mg) polymer were dissolved in 0.5 ml acetonitrile and the micelles were prepared as mentioned above. A second set of DTX or EVR or DDM were prepared using PEG_{4000}-*b*-PLA_{2200} polymer using the same procedure. Micelles were prepared in triplicate and the data is presented as Mean ± SD.

Particle size analysis

Particle size of polymeric micelles was measured by dynamic light scattering (DLS) using a Malvern Nano ZS (Malvern Instruments Inc., U.K.). Samples were diluted 20 times with deionized water to yield final polymer concentration of 1.5 mg/ml. The intensity of He-Ne laser (633 nm) was measured at 173°. All measurements were performed at 25 °C after pre-equilibration for 2 min. The particle size was measured in triplicates and Z-average size was reported as the Mean ± SD and polydispersity index (PDI).

Reverse phase high performance liquid chromatography (RP-HPLC) analysis for drug loading

The drug loading was determined using Shimadzu HPLC system consisting of LC-20 AT pump and SPD M20 a diode array detector. The analysis was performed using Zorbax C8 Column (4.6×75 mm, 3.5 µm) in isocratic mode with acetonitrile/water (62/38) containing 0.1% phosphoric acid and 1% methanol at a flow rate of 1 ml/min and injection volume of 10 µL. Column temperature was kept at 40 °C. The DTX and EVR peaks were monitored at 227 and 279 nm respectively. The retention times for DTX and EVR were 1.7 and 5.7 min respectively. All measurements were performed in triplicates.

***In vitro* drug release study from individual micelles and dual-drug loaded micelles**

DTX and EVR individual and were prepared as described above (preparation of drug loaded micelles section), and a sample of 2.5 mL was loaded into a Slide-A-Lyzer® (Thermo Scientific Inc.) dialysis 3.0 mL cassette with a MWCO of 7,000 g/mol. This MWCO was chosen to enable the free drug(s) along with the unassociated polymer molecules to diffuse freely out of the

cassette and thereby ensure sink conditions. Four cassettes were used in each experiment (n = 4). The cassettes were placed in 2.5 L of 10 mM phosphate buffer at pH 7.4, which was changed every 3 hr to ensure sink conditions and the temperature was maintained at 37 ^{o}C. The sampling time intervals were 0, 0.5, 1, 2, 3, 6, 9, 12, 24, and 48 hr. A sample of 150 µL at each time point was withdrawn, and the cassette was replenished with fresh 150 µL of buffer. Samples were analyzed by RP-HPLC for drug content. To evaluate drug release kinetics in more detail, the drug release data were curve-fitted assuming that the drug(s) were released by simple diffusion using a one phase exponential association equation. The time needed to reach 50 % of drug release, $t_{1/2}$ and first-order rate constant of each drug in individual or DDM as well as the goodness of fit were calculated. The curve fitting analysis was performed with GraphPad Prism version 5.04 for Windows, GraphPad Software, San Diego California USA, www.graphpad.com.

HUVEC cell proliferation assay

HUVEC cells were seeded at the density of 5,000 cells/well in 96 well plates and allowed to attach for 48 h at 37 °C. After incubation, cells were treated with individual or DDM. DTX concentration range was 0.02 - 2000 nM while EVR concentration range was 20 - 20,000 nM in individual micelle treatments. While for the DDM DTX:EVR (1:1) molar ratio the concentration range for each drug was from 0.02-200 nM. Cell viability was determined after 48 h by treatment with 20 µL of CellTiter-Blue® reagent followed by one hour of incubation at 37 °C and fluorescence ($560_{Ex}/590_{Em}$) signal was measured, all measurements were performed in quadruplicate. The drug concentration at 50% growth inhibition (IC_{50}) was determined by the *linearized median-effect plo*t using Compusyn software (Version 1.0, ComboSyn Inc., U.S.) (29). This software is based on Chou and Talay median-effect method in which the median-effect

equation is a general equation for dose-effect relationship derived from the mass-action law principle that takes into account the potency and the shape of dose-effect curve. The dose-effect relationship as shown by the mass action law is mathematically described below:

$$\frac{f_a}{f_u} = \left(\frac{D}{D_m}\right)^m$$

Where; f_a and f_u represent the effect while D is the dose causing the effect. The dose effect curve can be linearized by the *median effect plot* where $x=log(D)$ and $y=log(f_a/f_u)$

$$\log\left(\frac{f_a}{f_u}\right) = mlog\left(D\right) - mlog(D_m)$$

f_a: the fraction of cells affected upon drug treatment

f_u: the fraction of cells unaffected upon drug treatment, f_u=(1-f_a)

D: the dose of the drug

D_m: the dose that is required to produce a median effect (e.g., IC_{50}, ED_{50}, or LD_{50})

m: the slope of the line

Combination Index (CI) analysis

The combination effect of DTX and EVR loaded in DDM on HUVEC cells proliferation (see *HUVEC cell proliferation assay* section) was evaluated with Compusyn software using the Combination index (CI) analysis (29, 30) . CI value obtained from the software represents the effect of combination. CI value of 1 indicates additive effect, CI>1 indicates antagonism and CI<1 indicates synergism. CI value of DTX and EVR were computed using the following formula:

$$CI=\frac{(D)_1}{(Dx)_1}+\frac{(D)_2}{(Dx)_2}$$ Where is $(D_x)_1$ and $(D_x)_2$ are the inhibitory concentration of drug 1 and drug 2 alone respectively. $(D)_1$ and $(D)_2$ are the drug 1 and 2 concentration respectively. The data was represented as F_a-CI Plot (Chou-Talalay Plot) a plot of CI on y- axis as a function of effect level (F_a) on the x- axis.

***In vitro* endothelial tube formation assay**

Matrigel was thawed overnight at 4 °C in the ice bath and then 50 µL of solution was used to coat 96 well plates. The plates were then incubated at 37 °C for 60 minutes to ensure complete gelation of the matrix. HUVEC cells were then seeded into 96 well plates at a cell density of 20,000 cells/well and allowed to incubate for 18 h at 37°C. The total tube length and area were quantified using NIH ImageJ analysis software (31). Cells were treated with different concentrations of DTX (0.01, 0.1 and 1 nM), EVR (10, 100 and 1000 nM) individual micelles and DDM.

Migration Assay

HUVEC cell migration process was analyzed using xCELLigence RTCA DP instruments (Roche Applied Sciences, Germany). The system measures the electrical impedance which indicates the number of cells that migrated from the apical to the basolateral chamber in response to a chemoattractant. A change in electrical impedance was recorded in terms of *cell index* number. CIM-Plates 16 were coated with 20 µg/ml of fibronectin for 1 h. HUVEC cells were starved for 4 h with serum free medium and seeded on pre-coated fibronectin plates at a density of 15,000 cells/well. A change in electrical impedance was monitored every 10 min for 48 h. In the basolateral chamber, HUVEC cells complete medium was used as control and DTX, EVR and

DDM in complete medium as treatment groups were added in quadruplicates. The compiled data was presented as Mean ± SD. Significant differences between treatment group means was evaluated using one way ANOVA with Bartlett's test for equal variances and Bonferroni's multiple comparison test, using a threshold value (α) of 0.05.

Acute Toxicity Study

The acute toxicity of DTX, EVR individual and DDM was evaluated in six to eight-week-old FVB albino female mice (The Jackson Laboratory (Bar Harbor, ME) and housed in ventilated cages with free access to water and food. DTX, EVR or DDM were prepared freshly and reconstituted with saline and sterilized with 0.22 μm filter prior to injection. Six groups of mice (n=24; 4/group) were injected, i.v. (tail vein) with saline, DTX individual micelles, EVR individual micelle or DTX:EVR (1:1) DDM. The total number of injections for the treatment protocol was three and the injections were performed on days 0, 4 and 8 with the volume of injection between 80-180 μL. DTX individual micelles were injected at 40 or 30 mg/kg, EVR individual micelles were injected at 60 or 50 mg/kg and DDM were injected at total concentration of both drugs at 60 or 40 mg/kg (30 or 20 mg/kg for each drug).

Acute toxicity (dose limiting toxicity, DLT) was defined as the dose that causes a median body weight loss of ≥15% versus negative control (saline) and causes either remarkable change in general appearance or death. Mice with a weight loss ≥15% were euthanized because changes of this magnitude often indicate lethal toxicity. The maximum tolerated dose (MTD) was defined as dose level just below the DLT for a given formulation. Compiled data was presented as Mean ± SD. The animal work was conducted in compliance with NIH guideline and Institutional Animal Care and Use Committee policy in Oregon State University for End-Stage Illness and Pre-emptive Euthanasia based on Humane Endpoints Guidelines.

RESULTS

Drug loading and particle size analysis

Individual and dual-drug PEG-*b*-PLA micelles were formulated for DTX, EVR and their combination (Fig. 1). PEG_{4000}-*b*-PLA_{2200} micelles loaded with DTX were able to solubilize 1.74 ± 0.1 mg/mL mg/mL, while EVR loaded micelles were able to solubilize 2.00 ± 0.09 mg/mL (Fig. 2). The DTX-EVR dual-drug PEG_{4000}-*b*-PLA_{2200} micelles were able to load DTX and EVR at 1.91 ± 0.1 mg/mL at 2.0 ± 0.10 mg/ml respectively (Fig. 2). PEG_{2000}-*b*-PLA_{1800} micelles increased the water solubility of DTX to 1.93 ± 0.1 mg/mL (Fig. 2). Initial loading of PEG_{2000}-*b*-PLA_{1800} with EVR or DDM were similar but these micelles were not stable post 5 h at 25 ^{o}C as demonstrated by drug(s) precipitation. DTX in PEG_{2000}-*b*-PLA_{1800} and EVR in PEG_{4000}-*b*-PLA_{2200} individual micelles demonstrated excellent stability at 25 °C for more than 24 h at 25 ^{o}C with more than 98% drug was retained in solution. PEG_{4000}-*b*-PLA_{2200} DDM demonstrated higher stability at 25 ^{o}C for more than 24 h in comparison to PEG_{2000}-*b*-PLA_{1800} DDM. Stability studies also indicated that the PEG_{4000}-*b*-PLA_{2200} DTX micelles also were not stable due to drug precipitation. Therefore, all subsequent experiments were performed using PEG_{4000}-*b*-PLA_{2200} for EVR or DDM and PEG_{2000}-*b*-PLA_{1800} DTX micelles. PEG_{2000}-*b*-PLA_{1800} DTX micelle sizes were 18.05 ± 0.06 nm (PDI = 0.079 ± 0.013), while PEG_{4000}-*b*-PLA_{2200} EVR and DDM had sizes of 33.80 ± 0.05 nm (PDI = 0.113 ± 0.010) and 34.09 ± 0.24 nm (PDI = 0.137 ± 0.004) respectively (Fig. 3). All prepared micelles showed unimodal distribution with a PDI value of less than 0.2.

In vitro drug release study from individual micelles and DDM

The release profile of DTX and EVR from individual and DDM were evaluated in pH 7.4 buffer

at 37 ^{o}C over 48 hr by a simple dialysis method. DTX release profile from PEG_{2000}-*b*-PLA_{1800} individual micelles and PEG_{4000}-*b*-PLA_{2200} DDM is depicted in (Fig. 4A) with about 90% DTX released from both micelles over 48 hr. EVR release profile from PEG_{4000}-*b*-PLA_{2200} individual and DDM is illustrated in (Fig. 4B). The release of EVR from individual micelle after 48 hr was 60.0 ± 2.4 % while the EVR release from DDM after 48 hr was 49.2 ± 0.9 %. The time needed to reach 50 % of drug release ($t_{1/2}$), first-order rate constant of each drug in individual or DDM and the goodness of curve-fitting (r^2) were calculated and summarized in Table I. The goodness of curve-fitting (r^2) was in the range from 0.820 to 0.987, which means that the assumption for 1st order release was a good approximation to explain drug release from individual and DDM.

HUVEC cell proliferation assay

The antiproliferative effect of DTX, EVR individual and DDM were evaluated in HUVEC cells. The cytotoxicity of individual and DDM (1:1) micelles demonstrated a dose dependent decrease in cell viability. For all micelles the drug concentration at 50% growth inhibition (IC_{50}) was determined by the *linearized median-effect plo*t (Fig. 5). The IC_{50} values of DTX and EVR in individual micelles were 6.80 ± 0.67 nM and 18.57 ± 2.86 nM respectively (Fig. 6). The combination of DTX and EVR in DDM demonstrated strong dose dependent inhibition with IC_{50} value at 0.65 ± 0.11 nM (Fig. 5&6).

Combination Index (CI) analysis

To further analyze whether DTX and EVR combination are synergistic, additive or antagonistic, against HUVEC proliferation, the CI values for the various dosing ratios were calculated using Compusyn software. The calculated CI of DTX and EVR in DDM were well below 1.0 (Fig. 7) indicating significant synergistic antiproliferative effect against the HUVEC.

***In vitro* endothelial tube formation assay:** HUVEC were treated and cell differentiation was monitored *in vitro* by tube formation on matrigel matrix. HUVEC cells without treatment resulted in formation of regular capillary like tubular structures (Fig. 8A). DTX loaded PEG_{2000}-*b*-PLA_{1800} micelles at 1 nM reduced tube formation area by 40.14 ± 10.25 % (Fig 8B) while DTX micelles at 0.1 and 0.01 nM showed no significant reduction in the tube formation area compared to control. EVR loaded PEG_{4000}-*b*-PLA_{2200} micelles at 1000 nM showed reduction in tube formation areas by 53.87 ± 14.80 % (Fig 8C) while EVR micelles at 100 and 10 nM showed no significant reduction in the tube formation area compared to control. The DTX and EVR DDM demonstrated significant reduction in tube formation process in comparison to DTX or EVR individual micelles. DTX and EVR DDM combination at 0.5 nM and 500 nM respectively showed reduction in the tube formation area by 67.25 ± 7.60 % (Figure 8D).

Migration assay

To assess the effect of drug loaded polymeric micelles on endothelial cell migration; real time migration using xCELLigence RTCA DP Instrument was used. The cell index value indicates the number of cells that migrate in response to a chemoattractant. By plotting the *cell index* values over *time*, a signature real-time cellular migration (RTCM) profile can be generated to monitor HUVEC migration in real time. We observed dose-dependent significant inhibition of HUVEC migration with DTX loaded PEG_{2000}-*b*-PLA_{1800} micelles at different concentration below 1 nM and the lowest concentration of DTX significant inhibition in migration was 0.005 nM (Fig 9). In contrast, EVR PEG_{4000}-*b*-PLA_{2200} micelles did not show any significant inhibitory effect at 0.005 nM (Fig. 9). However, the EVR individual micelles showed strong inhibitory effect on

migration on HUVEC at different concentrations above 0.005 nM (data not shown). Interestingly, in case of DTX:EVR (1:1) DDM at 0.005 nM each (total of 0.01 nM) showed significant inhibition in cell migration compared to control and DTX individual micelle at 0.005 nM (Fig. 9). These findings confirm the synergistic/additive effect of DDM on HUVEC cell migration process.

Acute Toxicity Study

Mice were injected with EVR individual micelles at 60 and 50 mg/kg (n=8; 4/group). Mice injected with the 60 mg/kg EVR showed acute toxicity represented by lower extremity paralysis after the second injection (day 7). The second group of mice injected i.v., three times on day 0, 4, and 8 with EVR micelle at 50 mg/kg showed no sign of acute toxicity (Fig. 10A). DTX individual micelles were injected i.v., three times on day 0, 4, and 8 into 2 groups of mice (total n=8; 4/group) at 40 and 30 mg/kg. The first group injected with 40 mg/kg DTX showed acute toxicity after the third injection (day 16) represented by lost in weight > 15%. The second group injected with 30 mg/kg showed no sign of acute toxicity (Fig. 10B). DDM loaded with DTX:EVR (1:1) were injected i.v., three times on day 0, 4, and 8 into 2 groups of mice (total n=8; 4/group) at 30 and 20 mg/kg. The first group injected with 30 mg/kg DTX showed acute toxicity after the third injection (day 13) represented by lower extremity paralysis. The second group injected with 20 mg/kg showed no signs of acute toxicity (Fig. 10C). Treatment groups for individual and DDM showed no toxicity upon monitoring for an additional 39 days and all animal showed no signs of acute toxicity (data not shown) during this time. Thus, the MTD doses for the EVR, DTX and DDM were 50 mg/kg, 30 mg/kg and 20 mg/kg for each individual drug for a total of 40 mg/kg. For all the animals that showed acute toxicity, the experiments were

stopped immediately and the animals were humanly euthanized in compliance with the guideline stated above.

DISCUSSION

The main aim of our work is to develop a new treatment modality to overcome the acquired resistance to antiangiogenic therapy. This resistance can be potentially overcome by the implementation of co-treatment strategies, where multiple mechanisms of drug action can target neovascular angiogenic endothelial within the cancer tissue (32). Based on this concept, DTX and EVR, two drugs that inhibit angiogenesis through different pathways and the concurrent treatment with both drugs might produce additive/synergistic antiangiogenic effects (14, 17). To achieve this combination, we selected polymeric based nanoparticles as a vehicle for the dual delivery of DTX and EVR. It has been observed that PEG-*b*-PLA micelles can considerably improve the water solubility of DTX as well as other drugs such as rapamycin, 17AAG and etoposide (20, 21, 25). Therefore, and for the first time, we adapted this platform to formulate the combination of DTX and EVR into DDM along with EVR individual micelles. Two different DTX individual micelles were prepared as previously reported (20, 25) PEG_{2000}-*b*-PLA_{1800} DTX individual micelles were more stable than PEG_{4000}-*b*-PLA_{2200} micelle as demonstrated by lower drug precipitation presumably due to better drug-polymer compatibility. PEG_{2000}-*b*-PLA_{1800} individual micelles increased the solubility of DTX to 1.93 mg/mL which is comparable to the published data (25). PEG_{4000}-*b*-PLA_{2200} was used for EVR and DDM as enhanced stability was observed at room temperature due to better drug(s)-polymer interaction. We observed similar drug loading for DDM as compared to the individual drug loaded micelles. The ability of the block copolymers to load two drugs into the core at same concentrations as individual drugs is a behavior that needs further study, but these findings are consistent with earlier investigators

(20, 21). EVR micelles and DDM were larger in size ≈ 34 nm in comparison to DTX loaded micelles ≈ 18 nm. This difference in size was observed due to differences in the copolymer block lengths and molecular weights. Other investigators using different block copolymer for the preparation of micelles have reported similar behavior (36). It was reported that block copolymers of high molecular weight result in micelles of higher hydrodynamic radii. According to our findings, PEG_{4000}-*b*-PLA_{2200} always formed micelles of larger diameter irrespective of individual or multiple drug loaded micelles as compared to PEG_{2000}-*b*-PLA_{1800}. Therefore, the block copolymer chosen plays a significant role in determining the size of polymeric micelles formed.

The release of DTX and EVR form the individual and DDM *in vitro* was well fitted with one phase exponential association equation suggesting that the drug(s) release is a diffusion control process and not driven by micelle dissociation process (Table I). The release profile of DTX from PEG_{2000}-*b*-PLA_{1800} individual micelles and PEG_{4000}-*b*-PLA_{2200} DDM was almost identical with slight difference in the $t_{1/2}$ value (Table I and Fig. 4A). Surprisingly these results clearly showed that different polymer blocks as well as the presence of EVR have minimal effect on DTX release kinetic. On the contrary the release profile of EVR form PEG_{4000}-*b*-PLA_{2000} individual and DDM was influenced by the presence of DTX (Table I and Fig. 4B). DDM released 49.2 ± 0.9 % of total amount of EVR in 48 hr with $t_{1/2}$ = 17.44 and r^2 = 0.955. In contrast faster release was seen for EVR from PEG_{4000}-*b*-PLA_{2000} individual micelle with $t_{1/2}$ = 8.38 hr. Additionally more EVR was released from the individual micelles at 60.0 ± 2.4 %. The difference in the release profile between EVR micelles can be contributed to the burst effect in drug release that has been exhibited by the EVR individual micelle, in which about 20 % of the drug was release within the first 30 min of the release experiment (Fig. 4B). The burst effect

also affected the data goodness of fit to the suggested release equation r^2 = 0.820. This discrepancy in the release profile of the EVR from both micelles can be clearly contributed to the presence of DTX. It can be speculated that the presence DTX in the DDM enhanced the compatibility between the EVR and the polymer and thereby EVR release profile in the DDM was without burst effect.

DTX and EVR individual micelles exhibited dose dependent antiproliferative response on HUVEC cells (Fig. 6). The IC_{50} values for the individual micelle were slightly higher than the published data for the free drug at 0.5 nM for DTX and 0.12 nM for EVR (13, 16). The difference in IC_{50} values between the free drug and drug individual micelle is possibly due to the high stability of the micelles *in vitro* which results in lower free drug being available to exert its effect on the cells. The combination of the DTX and EVR (1:1) molar ratio in DDM exhibited strong synergistic inhibition on HUVEC proliferation over wide range of dosing (Fig. 6 & 7).

Endothelial tube formation involves multiple steps such as attachment, and migration prior to tube formation process. Tube formation is initiated with attachment of endothelial cells on the basement matrix and then is followed by migration of these cells towards each other to eventually form tubes (37). Our data has shown this process can be inhibited at various concentrations of DTX and EVR individual and DDM (Fig. 4). In the tube formation experiment, DTX at 1 nM showed significant reduction in the tube formation area compared to control, the result is in agreement with earlier findings were taxanes exert antiangiogenic effects at lower concentrations than their IC_{50} (11-13). EVR individual micelle significantly reduced the tube formation area at 1000 nM a higher concentration than its IC_{50}. The discrepancy in potency of EVR individual micelles in HUVEC proliferation and tube formation might be contributed to the micelle stability and to the short time frame for the tube formation experiment. Based on the

EVR release profile, PEG_{4000}-*b*-PLA_{2200} individual micelles release less than 40 % of the drug in 16 hr (Fig. 4B). Therefore we speculate that within the time frame of the tube formation assay (16 hr) only small portion of EVR was available to exert its effect on the cells. On the other hand in proliferation study HUVEC were incubated with the micelle for 48 hr thereby giving the micelle more time to release the free EVR and exert the effect. Interestingly the treatment of the HUVEC with a combination of DTX and EVR micelles at 0.5 and 500 nM respectively inhibited the tube formation significantly compared to DTX micelle alone at 1 nM, the data clearly shows that EVR can intensify the DTX inhibitory effect in HUVEC tube formation.

Real time migration assay with the DDM DTX:EVR, each at 0.005 nM (total of 0.01nM), demonstrated synergistic/additive inhibition in HUVEC cell migration (Fig. 9). It was observed that DTX individual PEG_{2000}-*b*-PLA_{1800} micelles at 0.005 nM concentrations. Meanwhile EVR loaded PEG_{4000}-*b*-PLA_{2200} micelles at 0.005 nM did not inhibited HUVEC migration; however the same micelle for EVR inhibited the cell migration at concentration above 0.005 nM. These results suggest that the combined treatment of DTX and EVR inhibits HUVEC cell migration by synergistic/additive response. Cell migration process is regulated through reorientation of centrosome in the intended direction of movement (38). It was also observed that change in microtubule plasticity can alter the reorientation of the centrosome (38). Based on this mechanism, in our study we postulate that EVR potentiates the antimigratory effect of DTX on endothelial cells (Fig. 9) by changing the microtubule plasticity. We observed that EVR enhanced the antimigratory activity of DTX at 0.005 nM a concentration at which individual DTX micelles has weaker inhibition on endothelial cell migration. Further studies are required to delineate the exact molecular mechanism behind the enhanced migratory activity in the case of DDM. Our study provides strong evidence that combined treatment of DTX and EVR DDM is

advantageous in comparison to individual drugs for antiangiogenic treatment due to its inhibition of four major cascade events in the angiogenic process.

The acute toxicity of the individual and DDM was examined in mice. The MTD for EVR individual micelles was 50 mg/kg which much higher than any published data, for example Iwase, et.al showed the MTD of liposomal EVR formulation in mice treated by intravenous injection was 5 mg/kg (24). The MTD for DTX micelles in our work was higher than Taxotere® at 20 mg/kg for similar dosing regimen (39). The DDM showed MTD at 20 mg/kg. For all micelles the MTD values were much higher than the required concentration to produce the anticancer or the antiangiogenic *in vivo* models as well as for clinical setting. In conclusion, we were able to formulate new micellar nanocarriers for EVR alone or in combination with DTX as a DDM. Also were able to show for the first time that the combination of DTX and EVR in DDM inhibited angiogenesis by affecting different cascade events in angiogenesis process with more potency than individual DTX or EVR micelles. Finally all micellar nanocarriers showed no acute toxicity at clinically relevant concentrations in mice.

Acknowledgment:

This study was supported by the grant from AACP New Pharmacy Faculty Research Award Program, Medical Research Foundation of Oregon New Investigator Grant and Oregon State University-Startup fund.

Drug(s) in micelle	first-order rate constant (hr^{-1})	$t_{1/2}$ (hr)	goodness of fit (r^2)
DTX	0.6931	10.00	0.986
EVR	0.0827	8.38	0.820
DTX	0.7824	8.86	0.987
EVR	0.0397	17.44	0.955

Table I: Curve fitting of *in vitro* drug(s) release from individual and DDM

Legend to Figures

Fig. 1: Schematic representation of individual and DDM

Fig. 2: Aqueous solubility of DTX in PEG_{2000}-*b*-PLA_{1800} individual micelles, EVR in PEG_{4000}-*b*-PLA_{2200} individual micelles and DTX-EVR DDM in PEG_{4000}-*b*-PLA_{2200} micelles (Mean ± SD, n=4).

Fig. 3: Particle size distributions (volume-weighted) for DTX in PEG_{2000}-*b*-PLA_{1800} individual micelles, EVR in PEG_{4000}-*b*-PLA_{2200} individual micelles and DTX-EVR DDM in PEG_{4000}-*b*-PLA_{2200} micelles.

Fig.4: *In vitro* drug release profiles of (A) DTX loaded in individual micelles and DDM (B) EVR loaded in individual micelles and DDM. (Mean ± SD, n=4).

Fig. 5: Linearized median-effect plot to calculate the IC_{50} (*Dm*) for DTX, EVR individual micelles and DDM. Linear regression was applied to the experimental data in order to obtain the value for *Dm*, and *m* parameters. The squared correlation coefficient r^2 is a measure of the overall precision of the linear regression, r^2 for DTX, EVR, DDM are 0.931, 0.939 and 0.993 respectively.

Fig. 6: IC_{50} values of DTX and EVR as individual micelles or DDM in HUVEC (Mean ± SD, n=4).

Fig. 7: *Fa-CI* plots of DTX and EVR combination in HUVEC cells. Cells were treated with DTX-EVR DDM at different concentrations

Fig. 8: Tube formation assay (a) Control, (b) DTX micelles (1 nM), (c) EVR micelles (1000 nM), (d) Co-administration of DTX (0.5 nM) and EVR (500 nM) micelles

Fig. 9: Real-time cellular migration profile (RTCM) for HUVEC cells treated with: DTX individual micelles (0.005 nM), EVR individual micelles (0.005 nM), and DDM with DTX 0.005 nM and EVR 0.005 nM. * Represents significant difference from untreated control and # represents significant difference between DTX individual micelle and DDM. (Mean ± SD, n=4)

Fig. 10: Relative body weight of mice over time after iv injection of DTX micelle, EVR micelle, or DDM (1:1) on days 0, 4, and 8. (A) EVR at 50 mg/kg, (B) DTX at 30 mg/kg, (C) DTX: EVR (1;1) DDM at 20 mg/kg for each drug total of 40mg/kg. *Dotted line* represents 15% of the starting average body weight. (Mean ± SD, n=4)

References

1. Longo R, Sarmiento R, Fanelli M, Capaccetti B, Gattuso D, and Gasparini G. Anti-angiogenic therapy: rationale, challenges and clinical studies. Angiogenesis. 2002;5(4):237-256.

2. Carmeliet P. Angiogenesis in health and disease. Nat Med. 2003;9(6):653-660.

3. Folkman J. Endogenous angiogenesis inhibitors. APMIS. 2004;112(7-8):496-507.

4. Li W, Hutnik M, Smith R, and Li V. Understanding Angiogenesis http://www.angio.org/ua.php (accessed April 16 2013).

5. Folkman J. Angiogenesis. Annu Rev Med. 2006;57(1-18.

6. Bocci Gand Loupakis F. The possible role of chemotherapy in antiangiogenic drug resistance. Med Hypotheses. 2012;78(5):646-648.

7. Guba M, von Breitenbuch P, Steinbauer M, Koehl G, Flegel S, Hornung M, *et al.* Rapamycin inhibits primary and metastatic tumor growth by antiangiogenesis: involvement of vascular endothelial growth factor. Nat Med. 2002;8(2):128-135.

8. Miller K D, Sweeney C J, and Sledge G W, Jr. Redefining the target: chemotherapeutics as antiangiogenics. J Clin Oncol. 2001;19(4):1195-1206.

9. Bocci G, Francia G, Man S, Lawler J, and Kerbel R S. Thrombospondin 1, a mediator of the antiangiogenic effects of low-dose metronomic chemotherapy. Proc Natl Acad Sci U S A. 2003;100(22):12917-12922.

10. Bocci G, Nicolaou K C, and Kerbel R S. Protracted low-dose effects on human endothelial cell proliferation and survival in vitro reveal a selective antiangiogenic window for various chemotherapeutic drugs. Cancer Res. 2002;62(23):6938-6943.

11. Hayot C, Farinelle S, De Decker R, Decaestecker C, Darro F, Kiss R, *et al.* In vitro pharmacological characterizations of the anti-angiogenic and anti-tumor cell migration properties mediated by microtubule-affecting drugs, with special emphasis on the organization of the actin cytoskeleton. Int J Oncol. 2002;21(2):417-425.

12. Wang J, Lou P, Lesniewski R, and Henkin J. Paclitaxel at ultra low concentrations inhibits angiogenesis without affecting cellular microtubule assembly. Anticancer Drugs. 2003;14(1):13-19.

13. Vacca A, Ribatti D, Iurlaro M, Merchionne F, Nico B, Ria R, *et al.* Docetaxel versus paclitaxel for antiangiogenesis. J Hematother Stem Cell Res. 2002;11(1):103-118.

14. Murtagh J, Lu H, and Schwartz E L. Taxotere-induced inhibition of human endothelial cell migration is a result of heat shock protein 90 degradation. Cancer Res. 2006;66(16):8192-8199.

15. Manegold P C, Paringer C, Kulka U, Krimmel K, Eichhorn M E, Wilkowski R, *et al.* Antiangiogenic therapy with mammalian target of rapamycin inhibitor RAD001 (Everolimus) increases radiosensitivity in solid cancer. Clin Cancer Res. 2008;14(3):892-900.

16. Lane H A, Wood J M, McSheehy P M, Allegrini P R, Boulay A, Brueggen J, *et al.* mTOR inhibitor RAD001 (everolimus) has antiangiogenic/vascular properties distinct from a VEGFR tyrosine kinase inhibitor. Clin Cancer Res. 2009;15(5):1612-1622.

17. Faivre S, Kroemer G, and Raymond E. Current development of mTOR inhibitors as anticancer agents. Nat Rev Drug Discov. 2006;5(8):671-688.

18. Adams M L, Lavasanifar A, and Kwon G S. Amphiphilic block copolymers for drug delivery. J Pharm Sci. 2003;92(7):1343-1355.

19. Oerlemans C, Bult W, Bos M, Storm G, Nijsen J F, and Hennink W E. Polymeric micelles in anticancer therapy: targeting, imaging and triggered release. Pharm Res. 2010;27(12):2569-2589.

20. Shin H C, Alani A W, Rao D A, Rockich N C, and Kwon G S. Multi-drug loaded polymeric micelles for simultaneous delivery of poorly soluble anticancer drugs. J Control Release. 2009;140(3):294-300.

21. Shin H C, Alani A W, Cho H, Bae Y, Kolesar J M, and Kwon G S. A 3-in-1 polymeric micelle nanocontainer for poorly water-soluble drugs. Mol Pharm. 2011;8(4):1257-1265.

22. Hasenstein J R, Shin H C, Kasmerchak K, Buehler D, Kwon G S, and Kozak K R. Antitumor activity of Triolimus: a novel multidrug-loaded micelle containing Paclitaxel, Rapamycin, and 17-AAG. Mol Cancer Ther. 2012;11(10):2233-2242.

23. Mazzaferro S, Bouchemal K, Gallard J F, Iorga B I, Cheron M, Gueutin C, *et al.* Bivalent sequential binding of docetaxel to methyl-beta-cyclodextrin. Int J Pharm. 2011;416(1):171-180.

24. Iwase Yand Maitani Y. Preparation and in vivo evaluation of liposomal everolimus for lung carcinoma and thyroid carcinoma. Biological & pharmaceutical bulletin. 2012;35(6):975-979.

25. Lee S W, Yun M H, Jeong S W, In C H, Kim J Y, Seo M H, *et al.* Development of docetaxel-loaded intravenous formulation, Nanoxel-PM using polymer-based delivery system. J Control Release. 2011;155(2):262-271.

26. Maciag T, Kadish J, Wilkins L, Stemerman M B, and Weinstein R. Organizational behavior of human umbilical vein endothelial cells. J Cell Biol. 1982;94(3):511-520.

27. Vailhe B, Vittet D, and Feige J J. In vitro models of vasculogenesis and angiogenesis. Lab Invest. 2001;81(4):439-452.

28. Kim S C, Kim D W, Shim Y H, Bang J S, Oh H S, Wan Kim S, *et al.* In vivo evaluation of polymeric micellar paclitaxel formulation: toxicity and efficacy. J Control Release. 2001;72(1-3):191-202.

29. Chou T-Cand Martin N. CompuSyn, *CompuSyn Software for Drug Combinations and for General Dose-Effect Analysis, and User's Guide*, ComboSyn, Inc., Paramus, NJ 2007.

30. Chou T Cand Talalay P. Quantitative analysis of dose-effect relationships: the combined effects of multiple drugs or enzyme inhibitors. Adv Enzyme Regul. 1984;22(0):27-55.

31. Schneider C A, Rasband W S, and Eliceiri K W. NIH Image to ImageJ: 25 years of image analysis. Nat Meth. 2012;9(7):671-675.

32. Pasquier E, Andre N, and Braguer D. Targeting microtubules to inhibit angiogenesis and disrupt tumour vasculature: implications for cancer treatment. Curr Cancer Drug Targets. 2007;7(6):566-581.

33. Pazdur R. FDA approval for doctaxel. http://www.cancer.gov/cancertopics/druginfo/fda-docetaxel (accessed April 21 2013).

34. Benjamin D, Colombi M, Moroni C, and Hall M N. Rapamycin passes the torch: a new generation of mTOR inhibitors. Nat Rev Drug Discov. 2011;10(11):868-880.

35. Pazdur R. FDA Approval for Everolimus. http://www.cancer.gov/cancertopics/druginfo/fda-everolimus#Anchor-Breast (accessed April 21 2013).

36. Huh K M, Lee S C, Cho Y W, Lee J, Jeong J H, and Park K. Hydrotropic polymer micelle system for delivery of paclitaxel. J Control Release. 2005;101(1-3):59-68.

37. Papetti Mand Herman I M. Mechanisms of normal and tumor-derived angiogenesis. Am J Physiol Cell Physiol. 2002;282(5):C947-970.

38. Hotchkiss K A, Ashton A W, Mahmood R, Russell R G, Sparano J A, and Schwartz E L. Inhibition of endothelial cell function in vitro and angiogenesis in vivo by docetaxel (Taxotere): association with impaired repositioning of the microtubule organizing center. Mol Cancer Ther. 2002;1(13):1191-1200.

39. Bradshaw-Pierce E L, Eckhardt S G, and Gustafson D L. A physiologically based pharmacokinetic model of docetaxel disposition: from mouse to man. Clin Cancer Res. 2007;13(9):2768-2776.

40. Grant D S, Williams T L, Zahaczewsky M, and Dicker A P. Comparison of antiangiogenic activities using paclitaxel (taxol) and docetaxel (taxotere). Int J Cancer. 2003;104(1):121-129.

Figure 1
Click here to download high resolution image

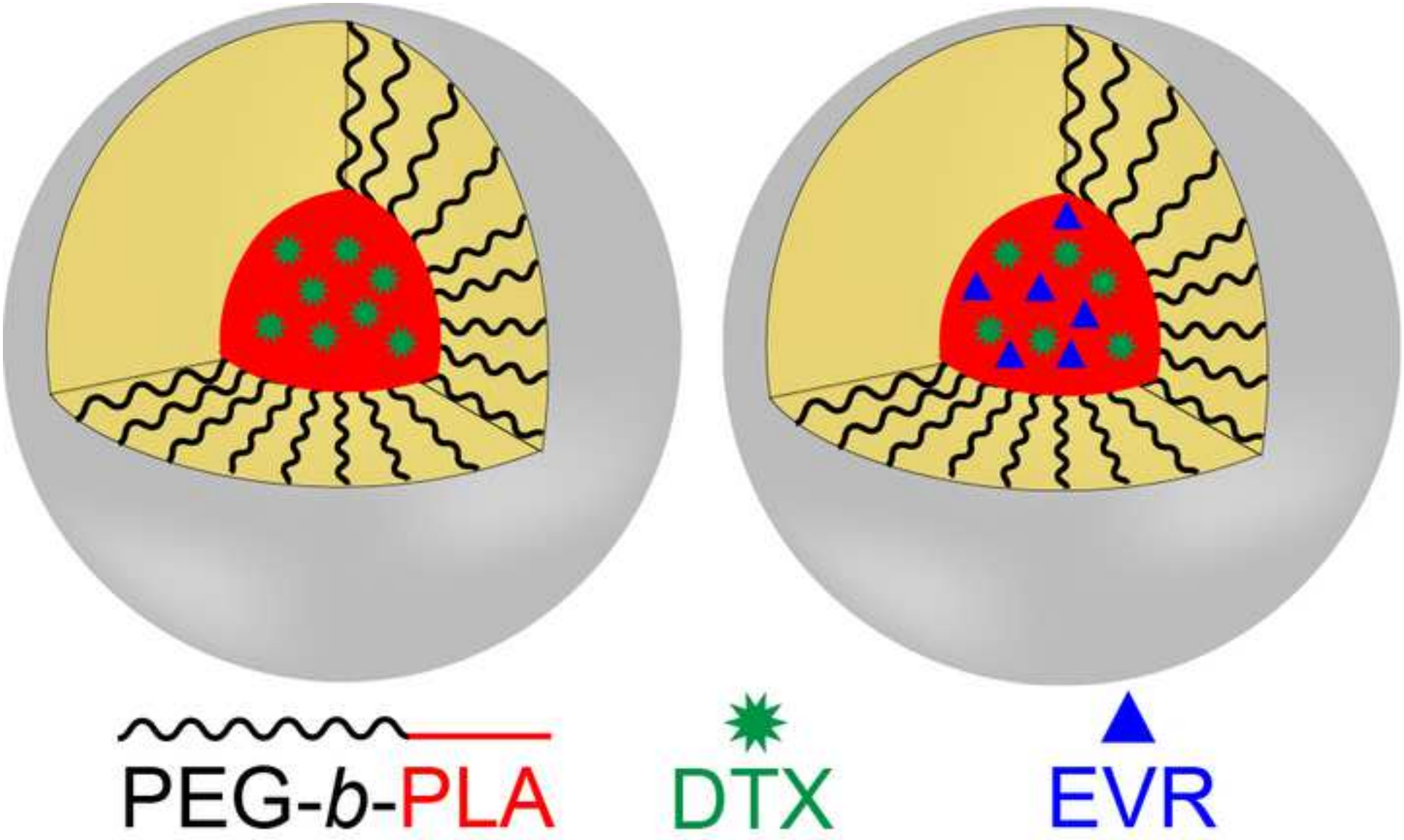

Figure 2
Click here to download high resolution image

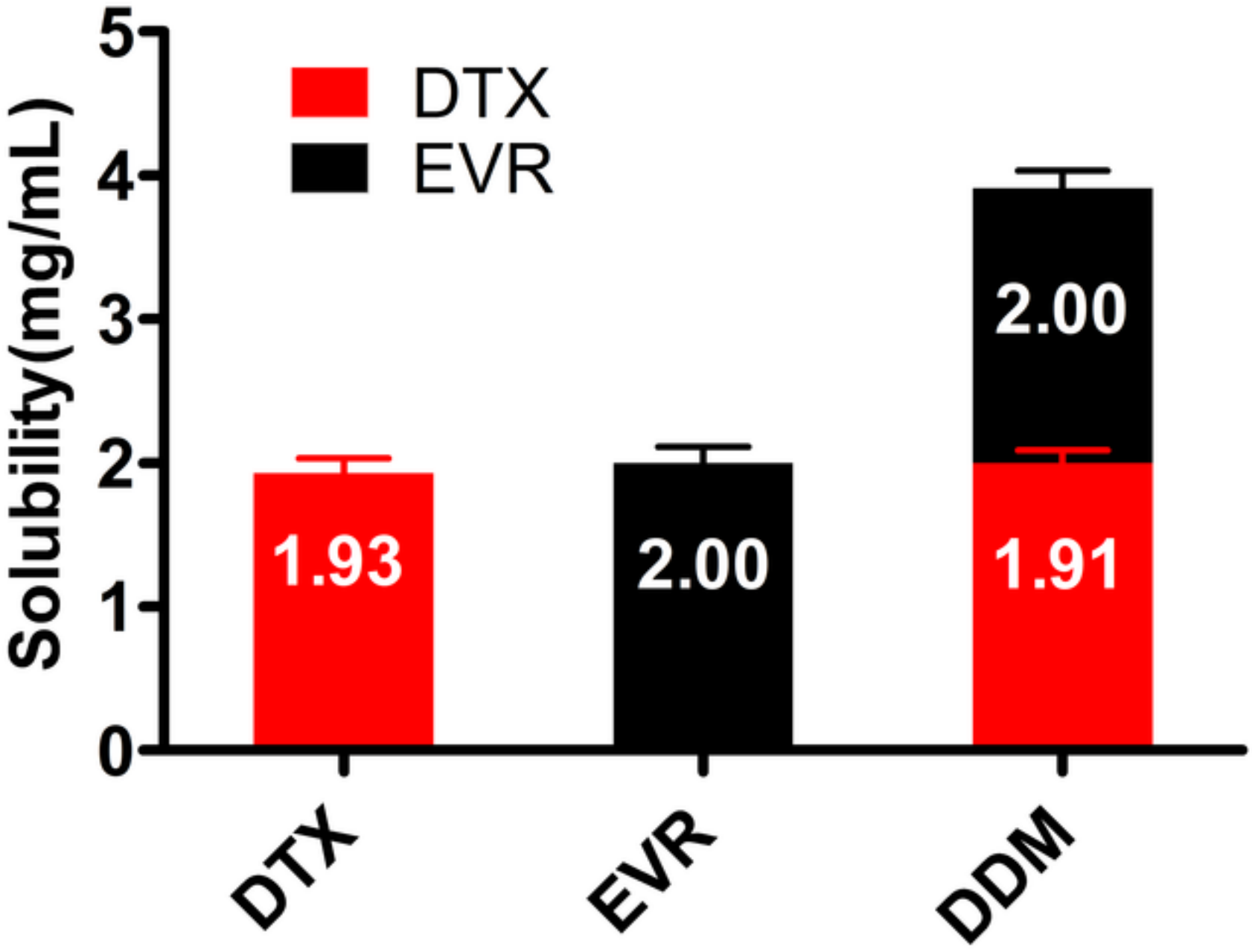

Figure 3
Click here to download high resolution image

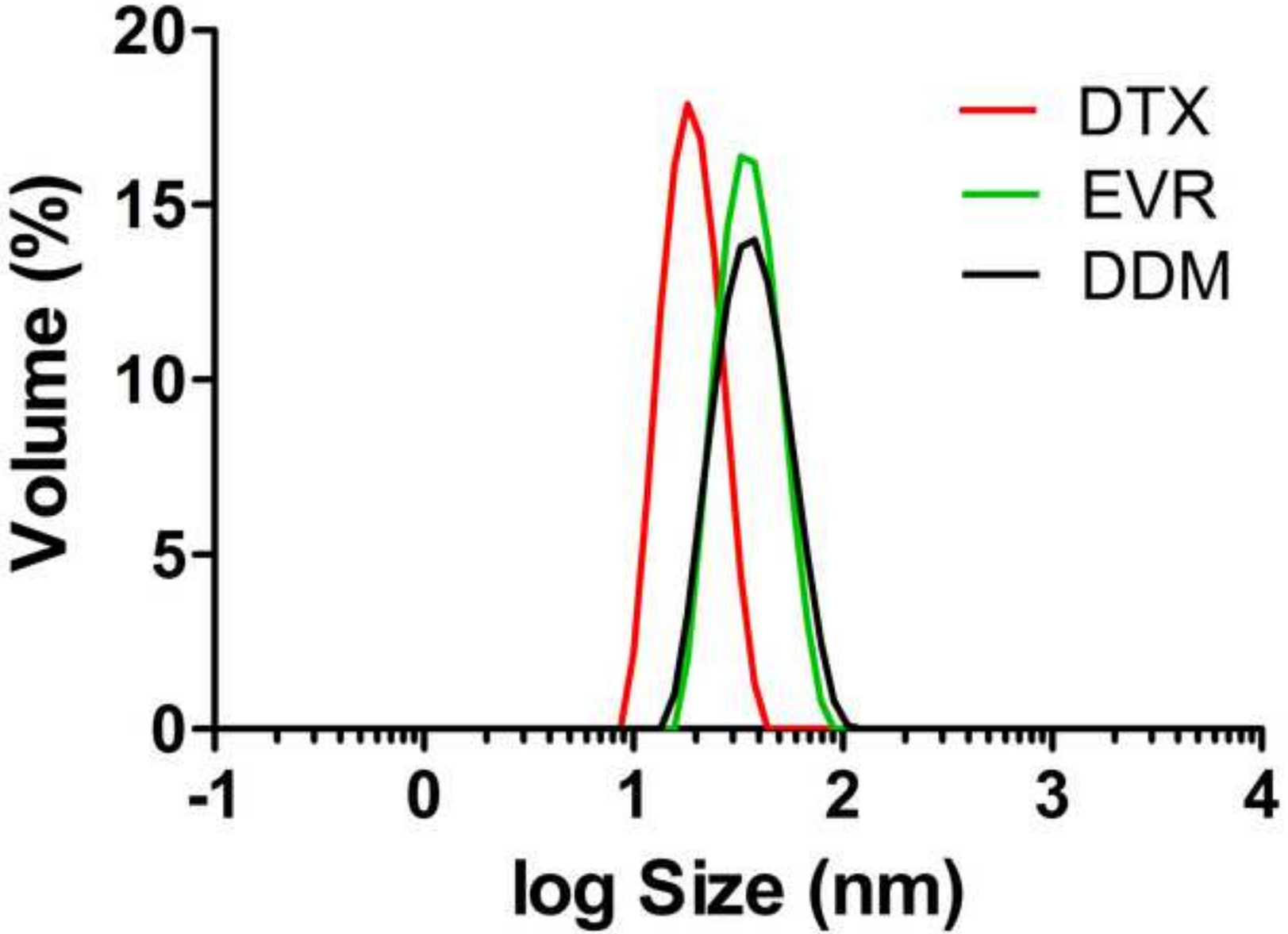

Figure 4_A
Click here to download high resolution image

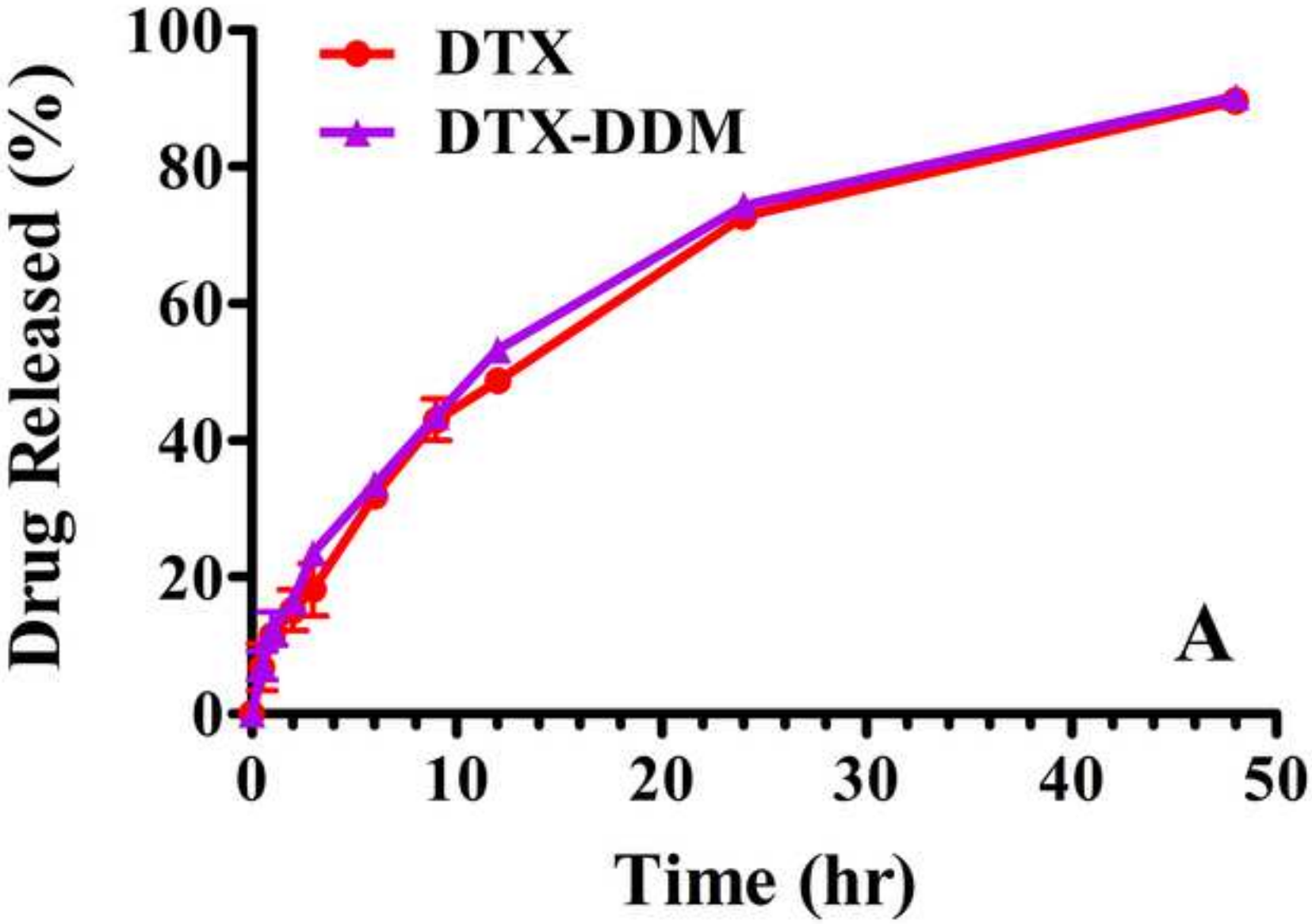

Figure 4_B
Click here to download high resolution image

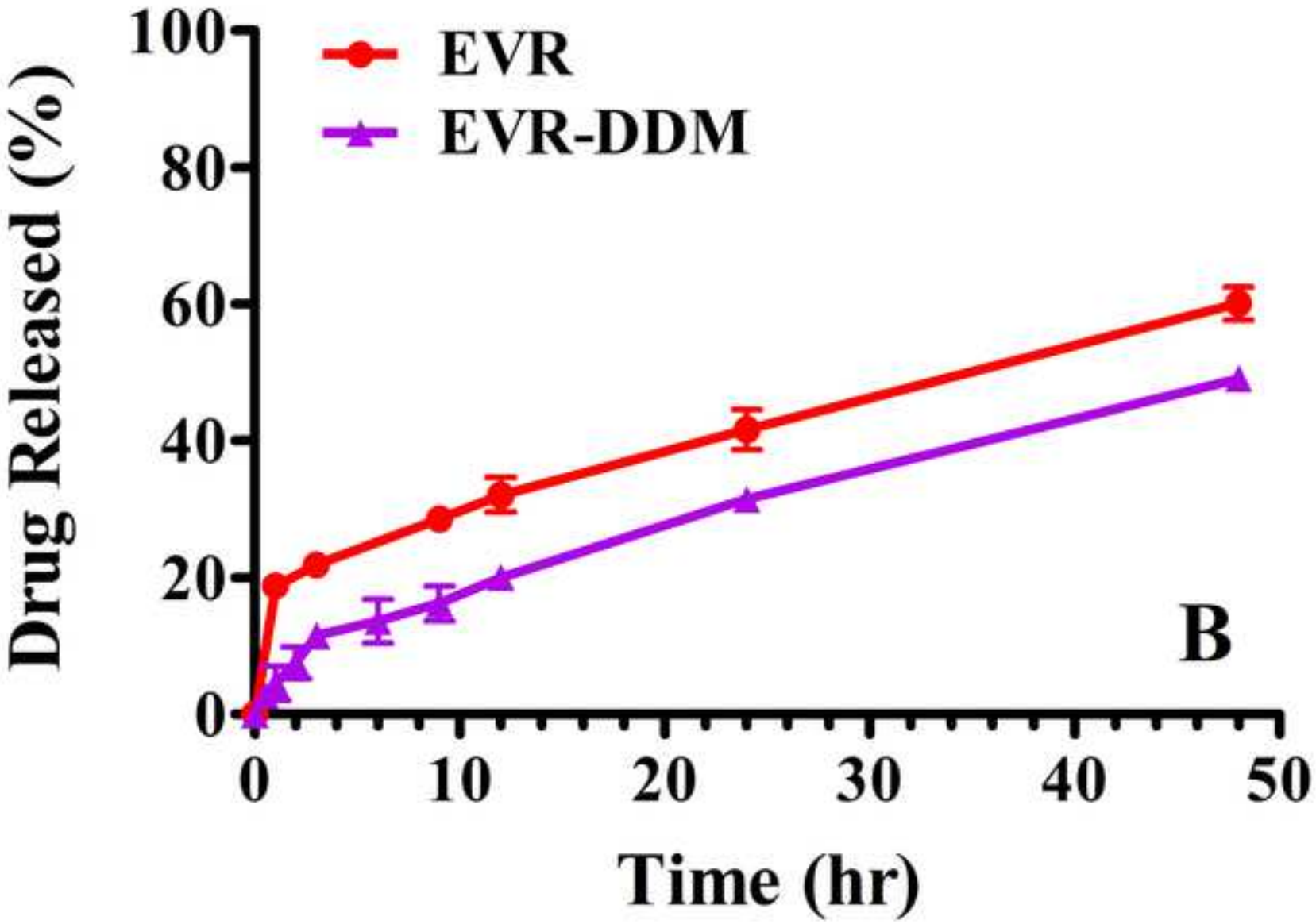

Figure 5
Click here to download high resolution image

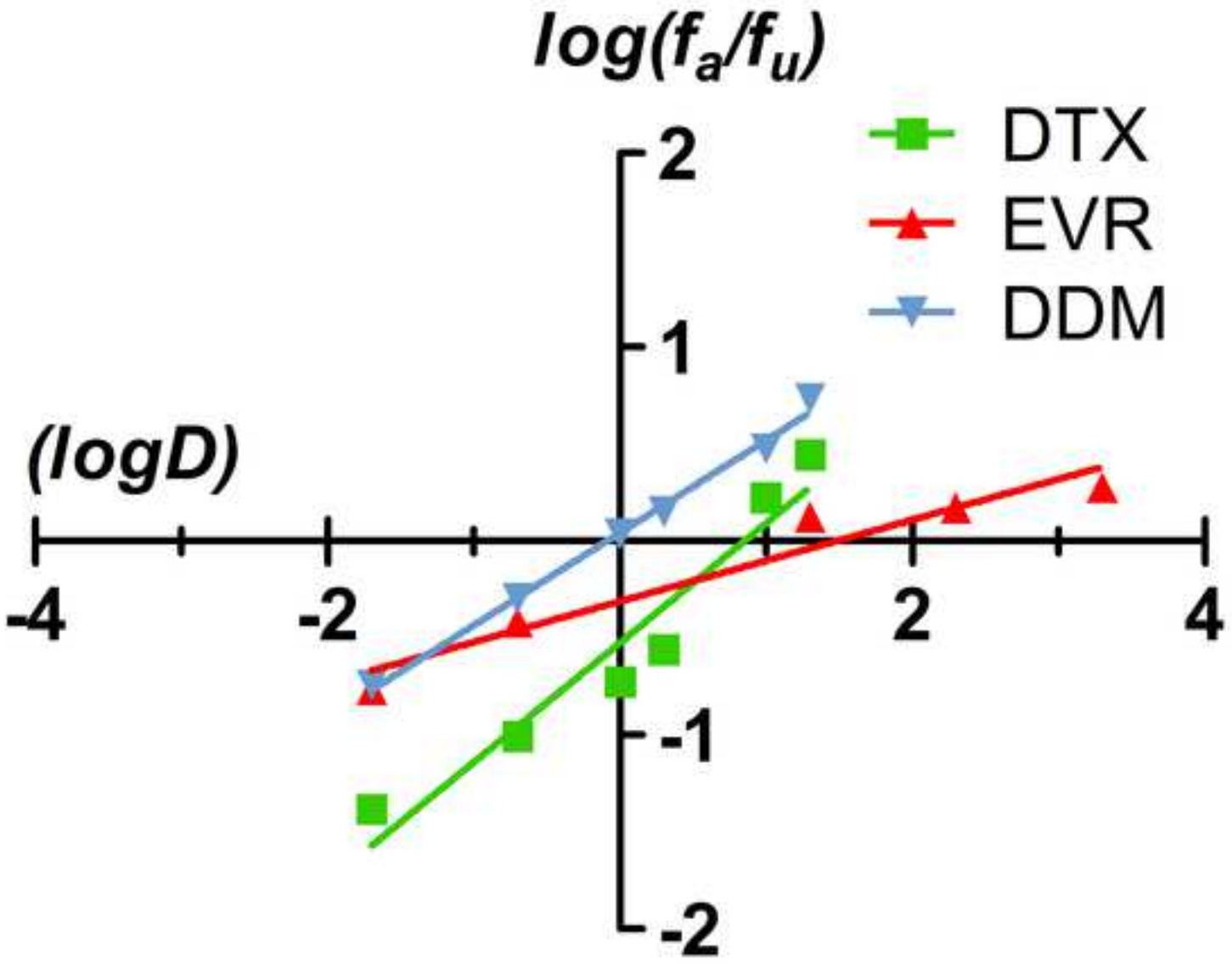

Figure 6
Click here to download high resolution image

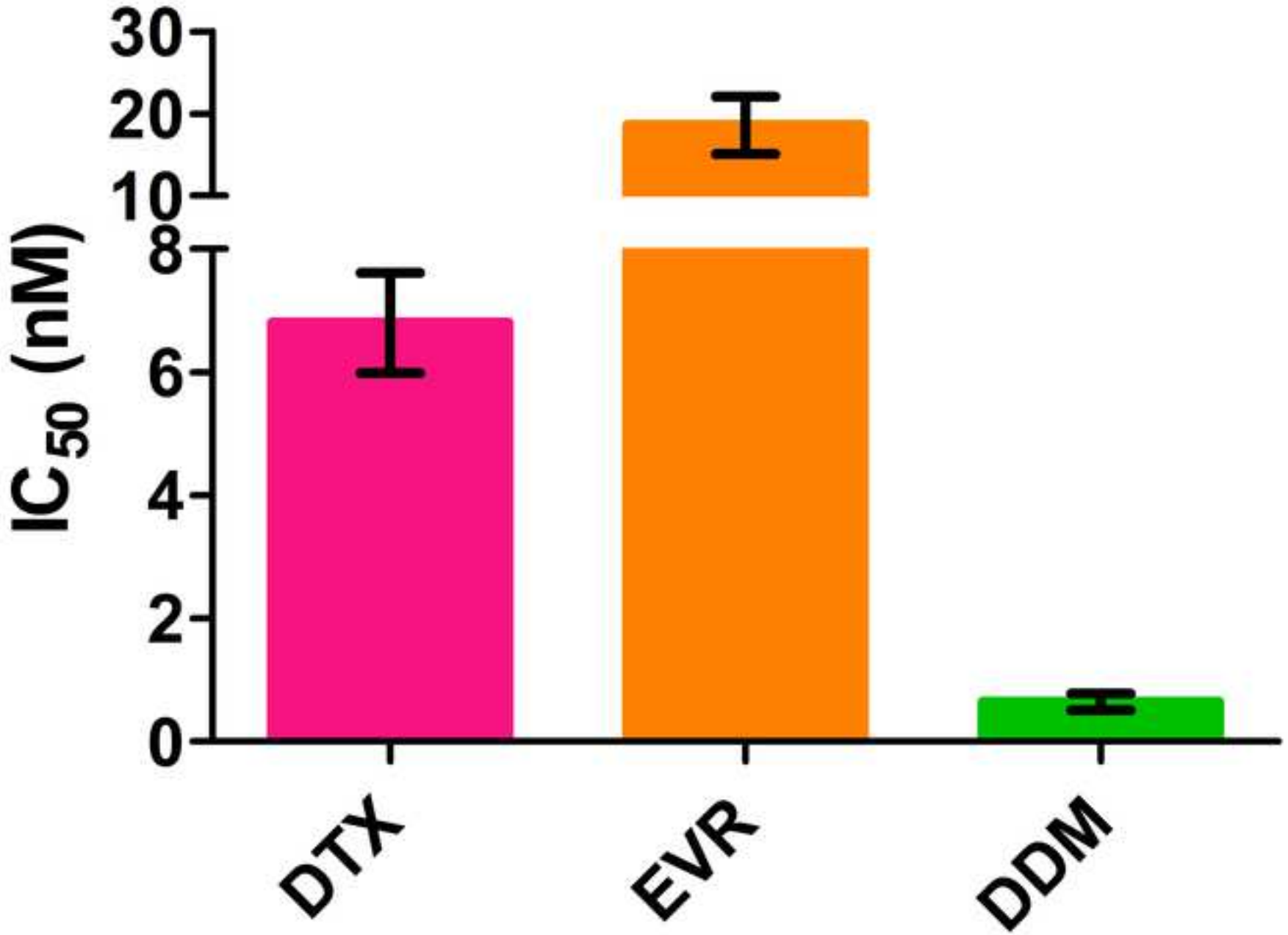

Figure 7
Click here to download high resolution image

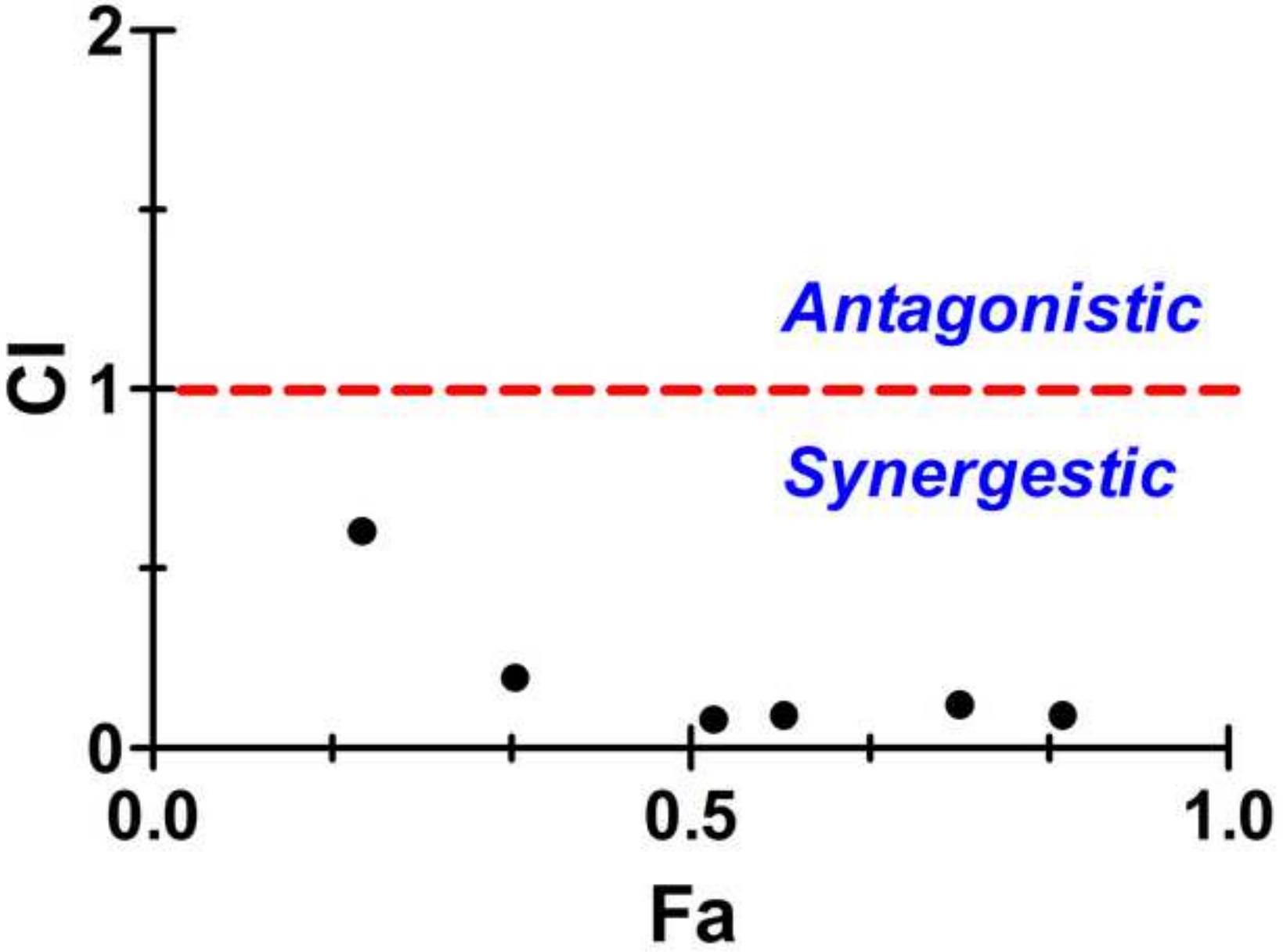

Figure 8
Click here to download high resolution image

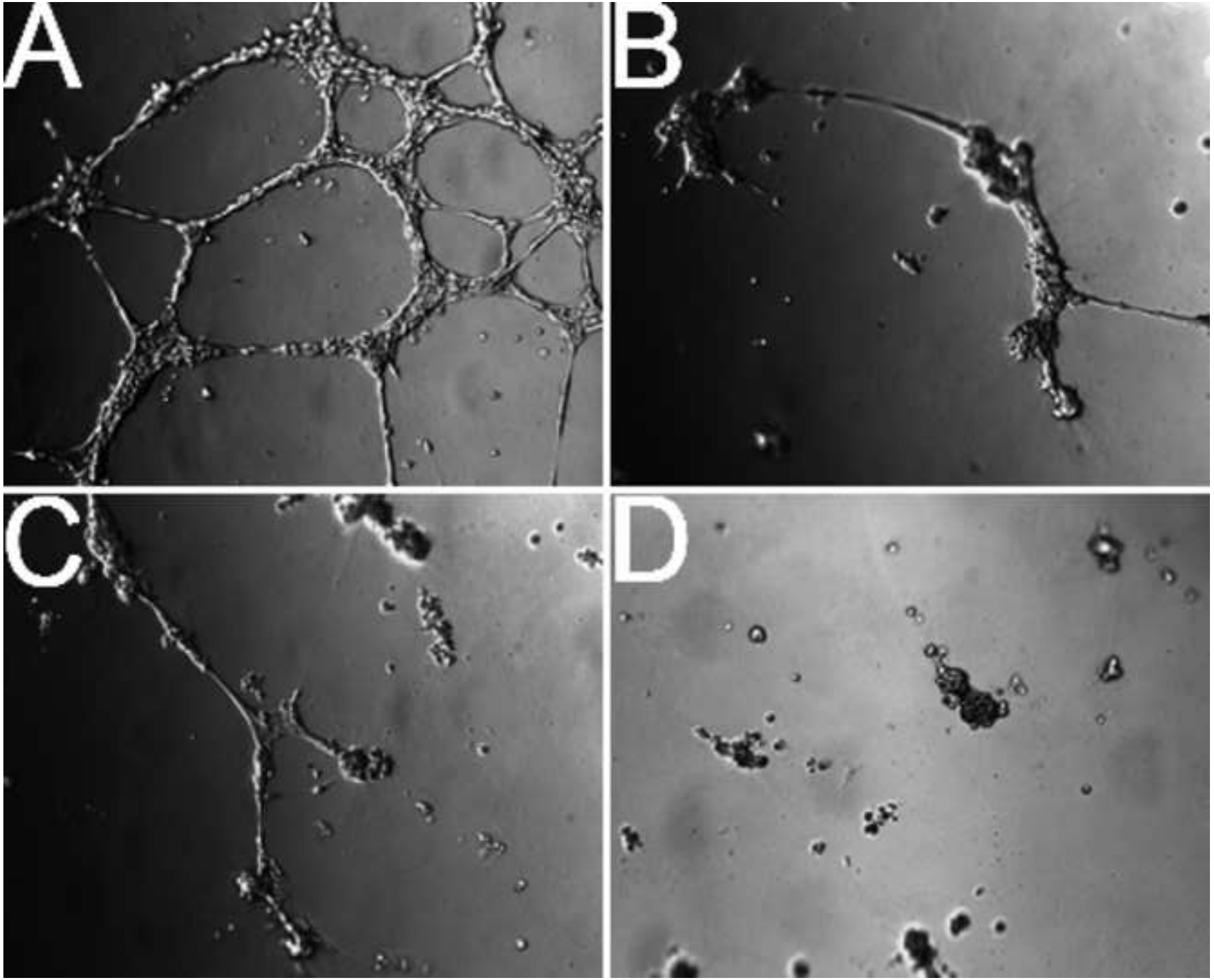

Figure 9
Click here to download high resolution image

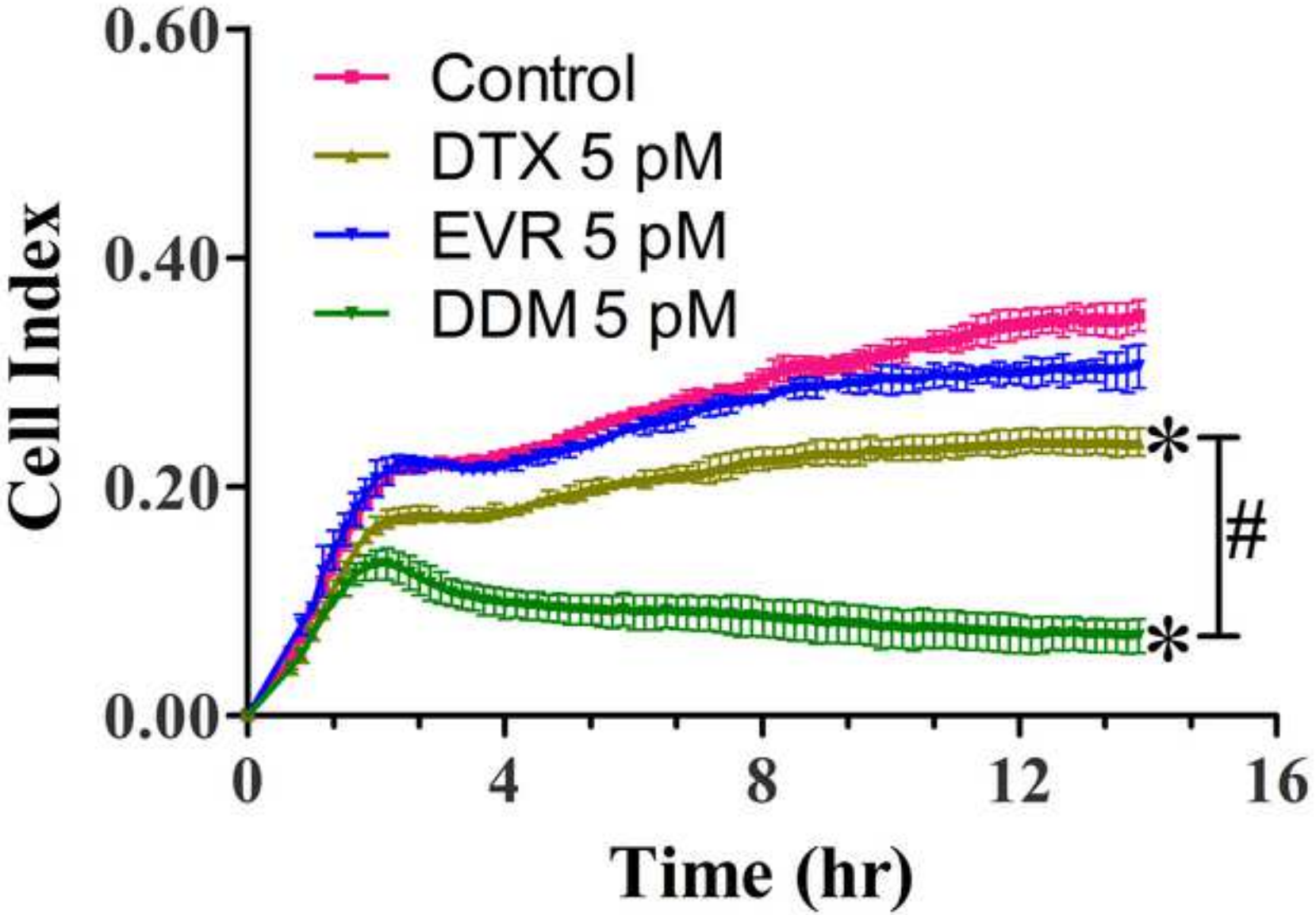

Figure 10_A
Click here to download high resolution image

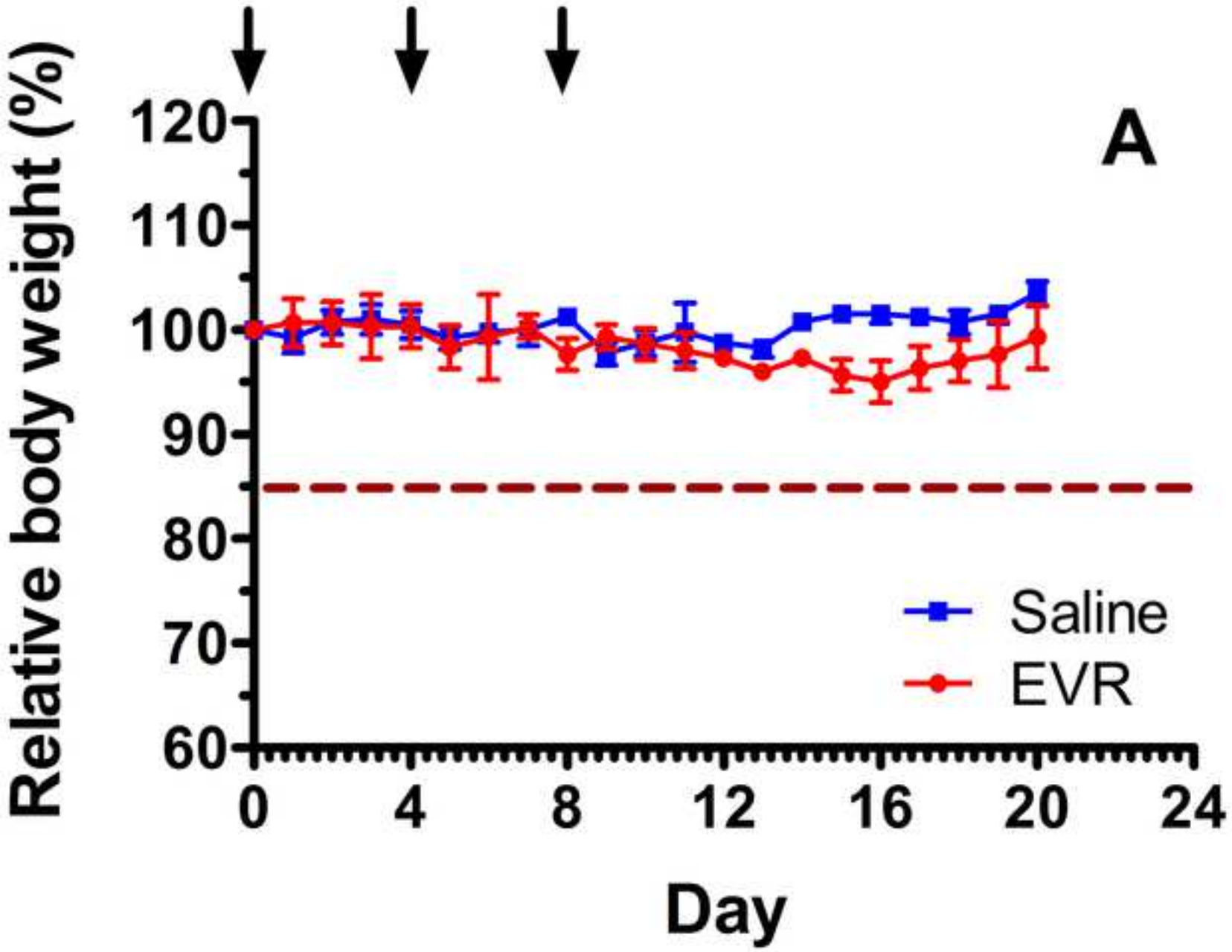

Figure 10_B
Click here to download high resolution image

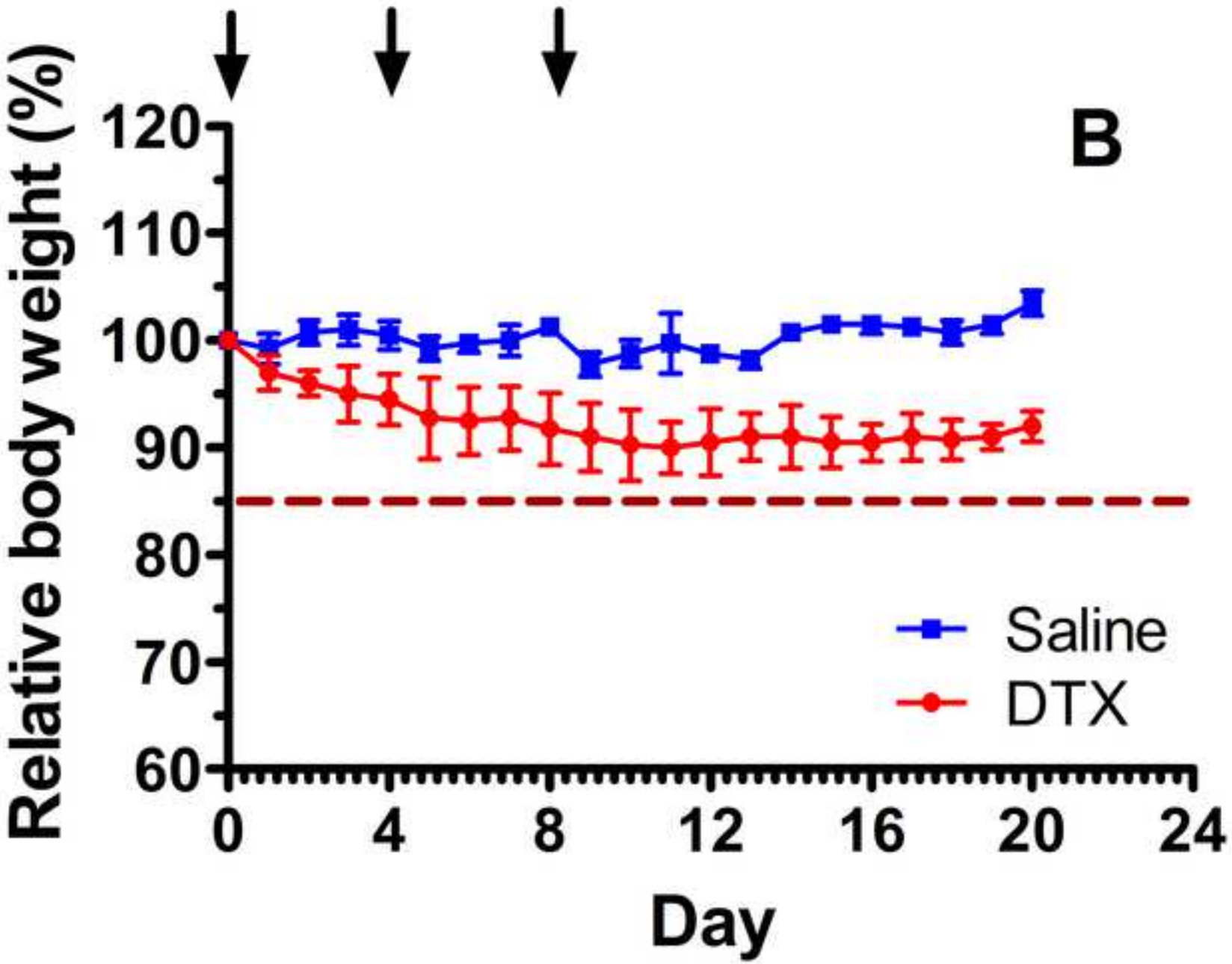

Figure 10_C
Click here to download high resolution image